Bull. Astr. Soc. India (2013) **41**, 159–172

Photometric study of hot contact binaries in SMC

D. Shanti Priya,[1*] K. Sriram,[2], K.Y. Shaju,[3] and P. Vivekananda Rao[1]

[1]*Department of Astronomy, Osmania University, Hyderabad 500 007, India*
[2]*Korea Astronomy and Space Science Institute, Daejeon 305-348, Republic of Korea*
[3]*Cochin University of Science and Technology, Cochin, Kerala, India*

Received 2012 April 18; accepted 2013 February 22

Abstract. In this paper we present the analysis of twenty hot contact binary systems in the Small Magellanic Cloud using the Wilson-Devinney method and their properties are discussed in context of TRO model.

Keywords : stars: binaries: eclipsing – stars: binaries: close

1. Introduction

The study eclipsing binaries (EBs) is an important tool to determine the physical properties of stars (Torres et al. 2009; Guinan 1993; Popper 1967). The orbital motion from the radial velocity curves along with the shape of the eclipse obtained from the light curves can be entirely explained by the geometry and the gravitational laws of the system (see Hilditch 2001). EBs are often being used to measure the distance of the host body (Munari et al. 2004; Kaluzny et al. 1998; Ribas et al. 2005). Despite of the best efforts an uncertainty of about 20%–30% still exists between the observed and theoretical radii possibly caused by metallicity, magnetic activity and mass exchange effects (Lopez-Morales 2007).

Contact binaries belong to one of the classes of EBs where two stars are surrounded by a common convective envelope, most probably exchanging mass and energy. The primary model for contact binaries was developed by Lucy (1968, 1976) and Flannery (1976) consisting of two main-sequence stars, where each component's radius is oscillating around its critical Roche lobe. During the evolution, matter flows from the primary to the secondary forming an envelope over it, blocking the inherent thermal flux of the secondary. Later, this envelope expands on a thermal time scale and specific entropy of both the stars becomes equal. As the secondary Roche lobe fills, mass/energy transfer from the primary stops and the star shrinks until the cycle of the thermal

*email: astroshanti@gmail.com

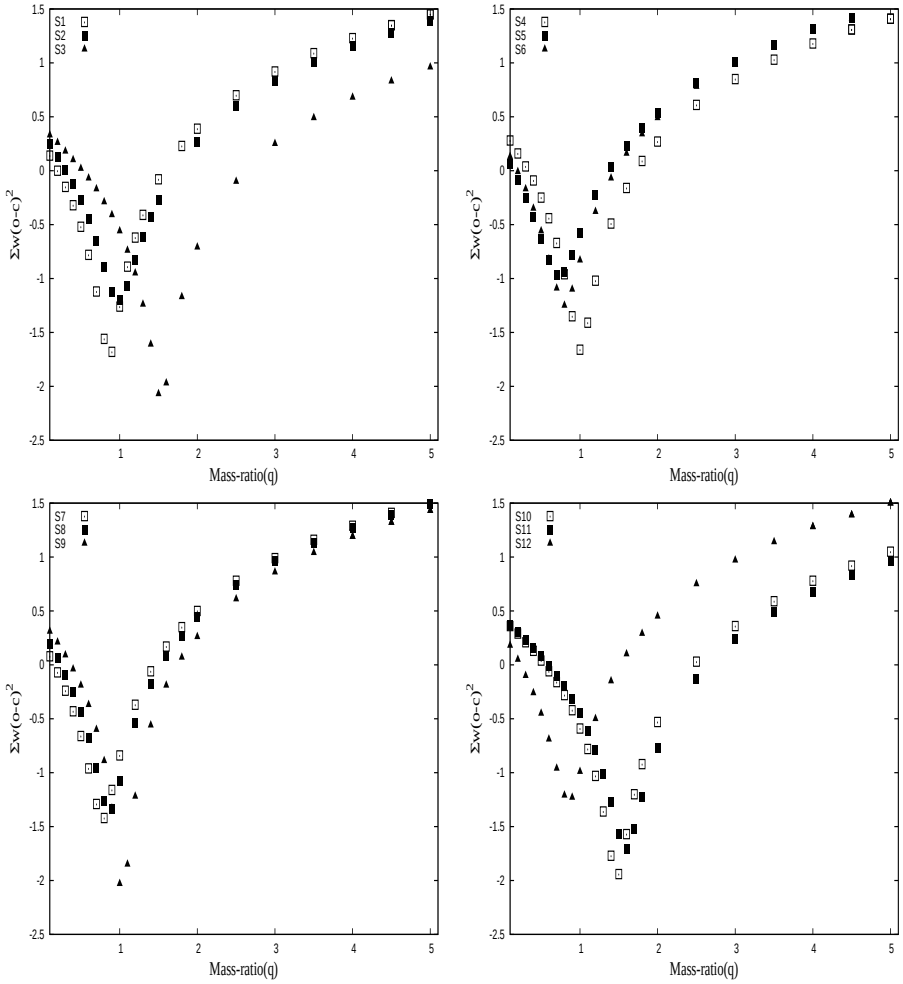

Figure 1. The figures show the q vs $\Sigma w(o\text{-}c)^2$.

relaxation oscillations (TROs) repeats. The overall TRO cycle drives the binary system from a semi-detached to a contact phase. It is observed that the low mass companion is found to be over-sized compared to the ZAMS (Zero Age Main Sequence) radius either due to the convective energy transfer from the massive component (Yakut & Eggleton 2005) or due to the depletion of hydrogen core (Paczynski et al. 2007; Stepien 2009); however the exact reason is unknown. Theoretical studies show that gradually the two stars merge to form a single star (Stepein 2006) but the uncertainty remains in the understanding of angular momentum removal mechanisms. In a few contact binaries high temperature differences between two binary companions were observed which could be due to an off-contact phase of thermal relaxation oscillation (TRO) model, an important observational evidence of TRO model (Martignoni et al. 2009; Rucinski & Duerbeck

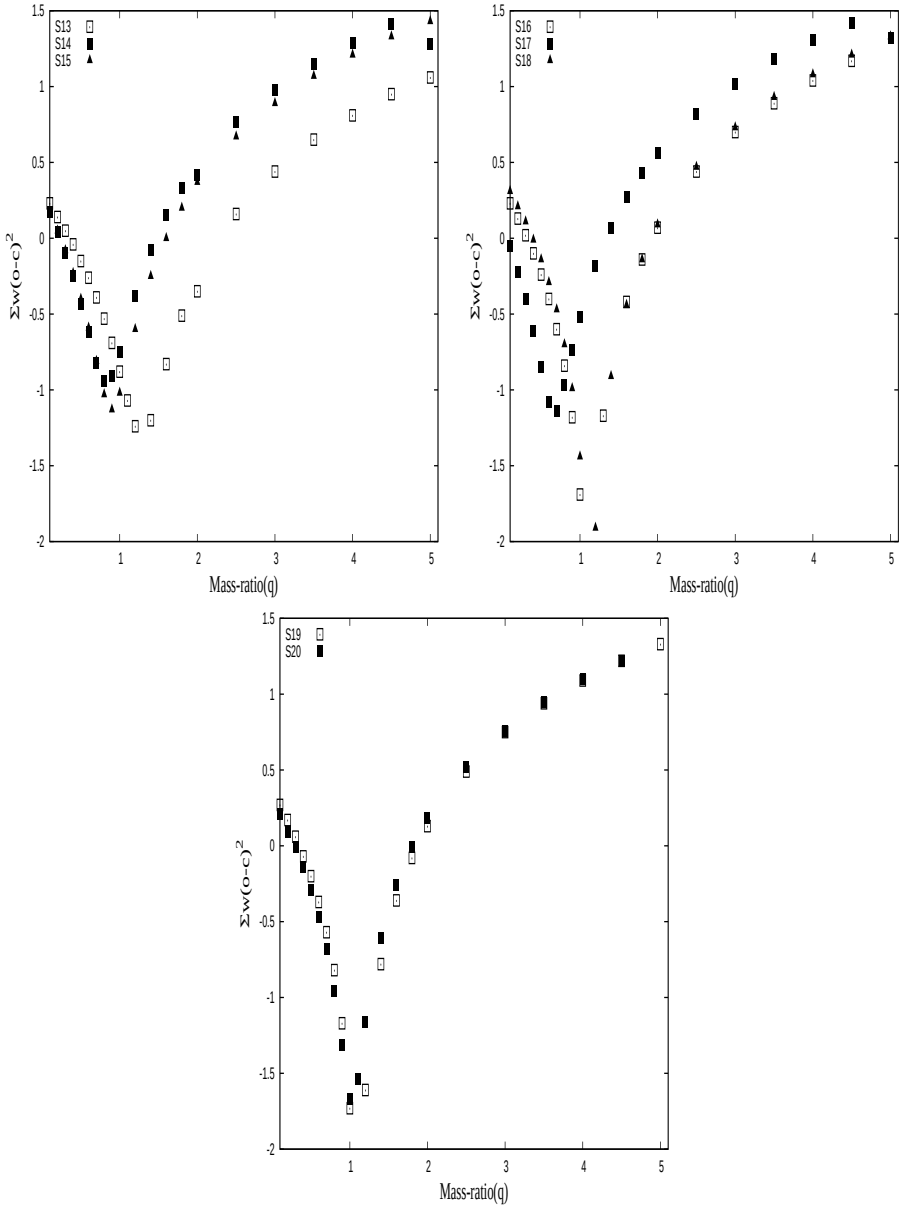

Figure 2. The figures show the q vs $\Sigma w(o\text{-}c)^2$.

1997). On the other hand very few hot contact binaries have been studied compared with the cool contact binaries.

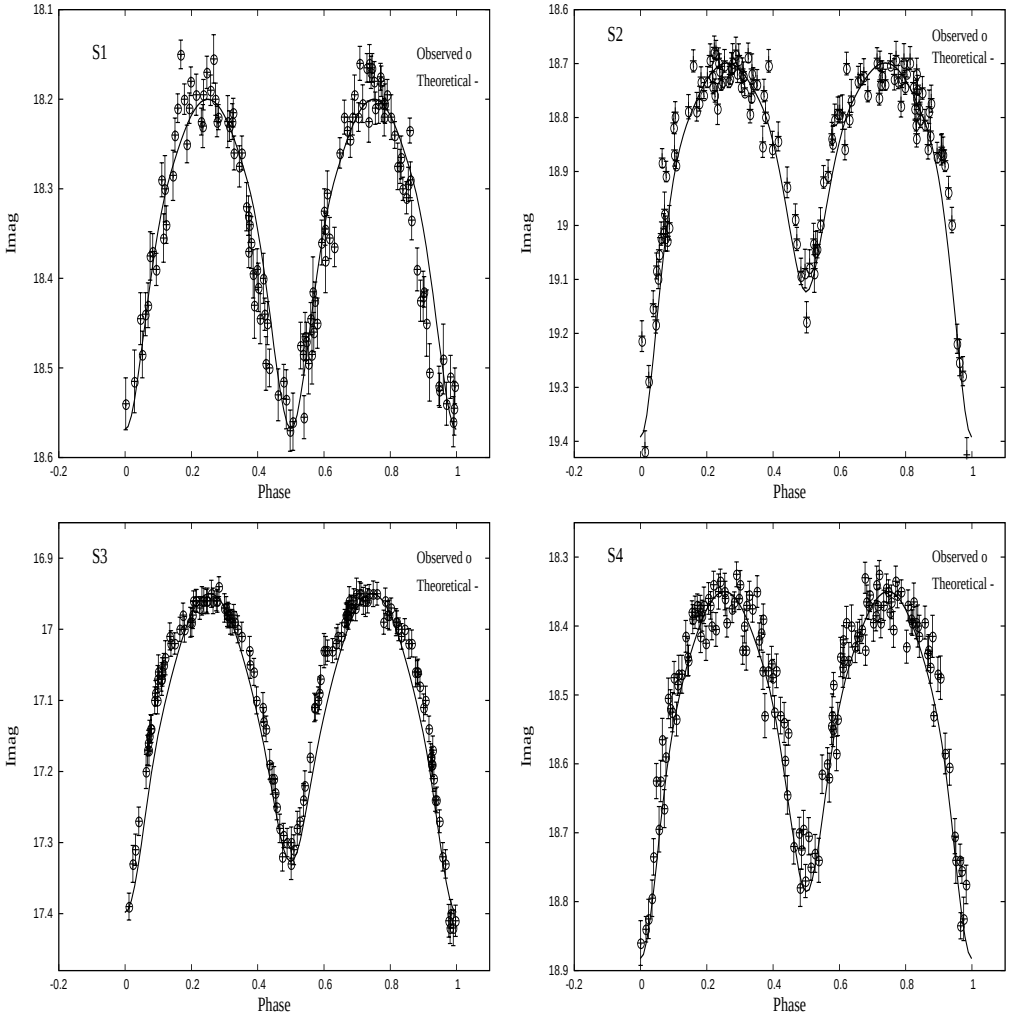

Figure 3. The figures show the best fits to the I passband light curves for the variables S1, S2, S3 and S4 in SMC.

Similar work was carried out on the contact binaries in LMC (Shanti et al. 2011), ω Centauri (Ravi Kiron, Sriram & Vivekananda Rao 2011a), Be 39 (Sriram, Ravi Kiron & Vivekananda Rao 2009; Ravi Kiron, Sriram & Vivekananda Rao 2011c), NGC 2539(Ravi Kiron, Sriram & Vivekananda Rao 2012), NGC 7789 (Sriram & Vivekananda Rao 2010 ; Ravi Kiron, Sriram & Vivekananda Rao 2011b), and NGC 6791 (Rukmini et al. 2005), Be 33 (Rukmini & Vivekananda Rao 2002). We have used the Wilson-Devinney program version 2003 (Wilson & Devinney 1971; Van Hamme & Wilson 2003) in order to derive the various photometric elements and put constraints on the mass-ratio parameter. In this paper, twenty hot contact binaries have been

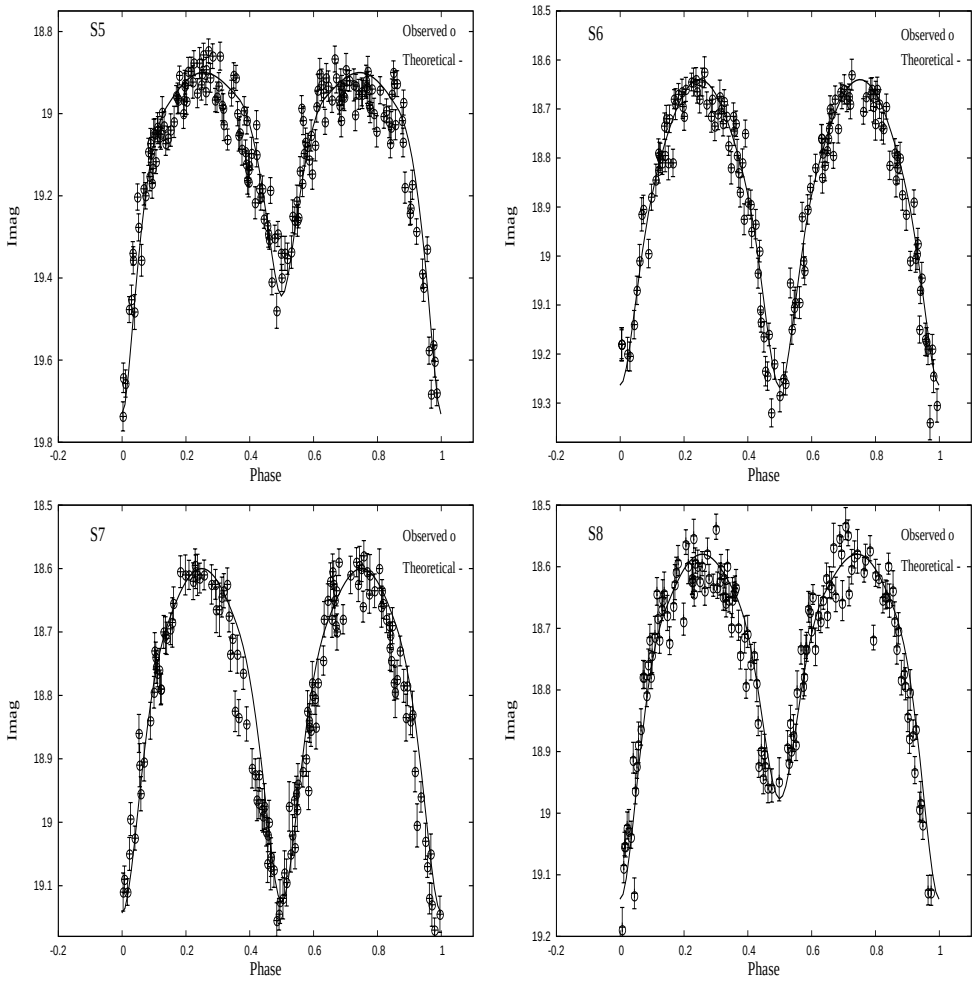

Figure 4. The figures show the best fits to the I passband light curves for the variables S5, S6, S7 and S8 in SMC.

selected in the field of the Small Magellanic Cloud (SMC), originally obtained from the Optical Gravitational Lensing Experiment (OGLE) II survey (Udalski et al. 1997). We have found that a few of the systems have large temperature differences, and we discuss their properties in the context of the TRO model.

2. Data selection and analysis

The OGLE II survey by Udalski et al. (1997) has provided the catalog of B, V and I magnitudes of 1402 eclipsing binaries in SMC and the data was available in public domain for further analysis.

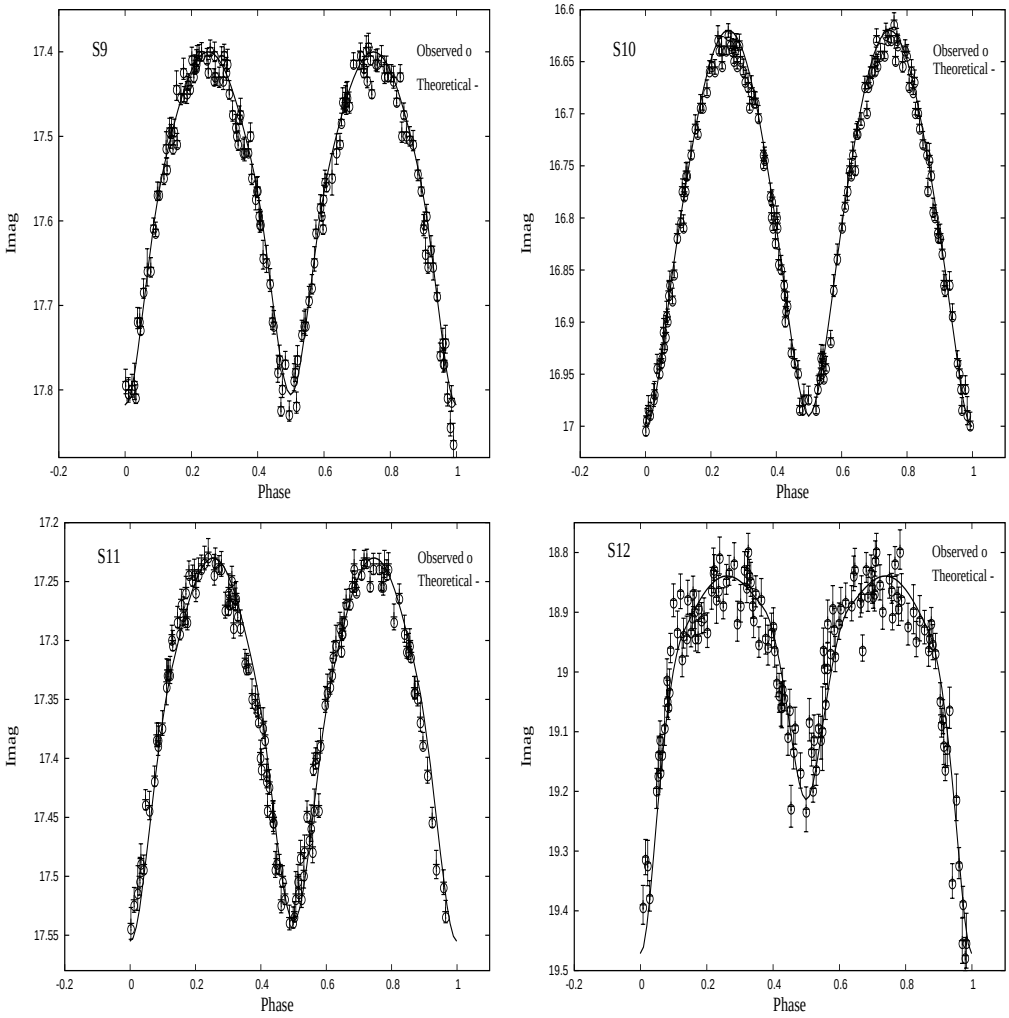

Figure 5. The figures show the best fits to the I passband light curves for the variables S9, S10, S11 and S12 in SMC.

Further work by Wyrzykowski et al. (2003) had found 733 EA type, 570 EB type and 150 EW type stars. In general the periods of contact binaries are less than a day and hence we have selected twenty variables with the criteria (see Table 1), period less than or equal to 0.8^d, I passband light curve amplitude ≥ 0.4 with minimum scatter of < 0.05 and complete coverage of the light curve with prominent primary and secondary depths. We found that the selected variables are hot ($\sim$ 10000 K) based on V-I colour and such systems are rarely being studied. The Wilson-Devinney program version 2003 was used (Wilson & Devinney 1971; Van Hamme & Wilson 2003) to obtain the various photometric elements.

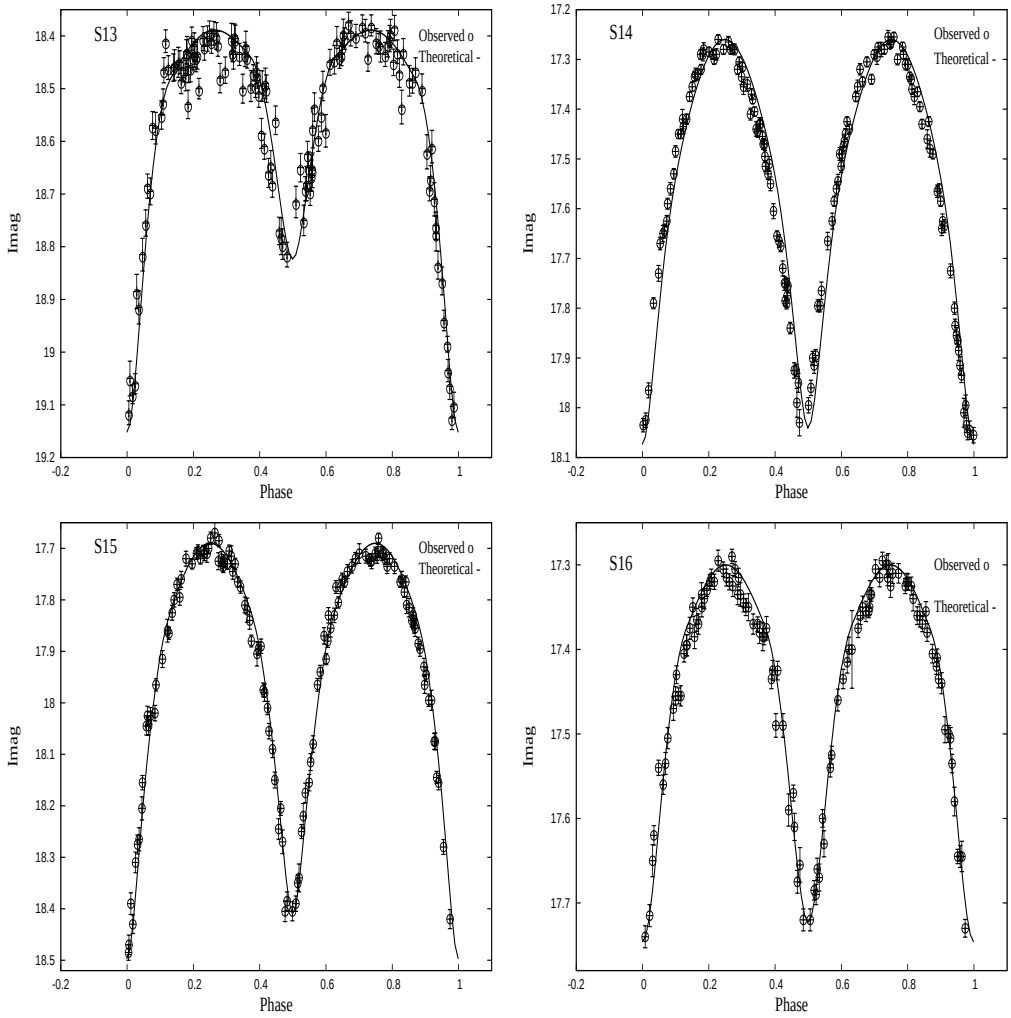

Figure 6. The figures show the best fits to the I passband light curves for the variables S13, S14, S15 and S16 in SMC.

3. Photometric solutions

We have re-calculated the periods of the selected variables using SigSpec introduced by Reegen (2007) and it was found that the derived periods are similar to the ones given in the OGLE database. The photometric solutions were obtained by using the latest Wilson-Devinney code, which synthesizes light curves using a model of stellar surfaces based on Roche geometry. The program we used is with an option of non-linear limb darkening via a square root law along with many other features (Wilson& Devinney 1971; Van Hamme & Wilson 2003). Initially all the

Table 1.

Star ID	OGLE star ID	Period (d)	I mag	V-I	Temperature (K)
S1	OGLE004111.95-731927.1	0.5546	18.13	0.05	9351
S2	OGLE004459.65-732122.4	0.6651	18.68	0.27	8004
S3	OGLE004538.22-725617.5	0.7625	16.93	-0.12	11400
S4	OGLE004617.81-732811.9	0.6057	18.3	0.08	4088
S5	OGLE004710.14-731045.8	0.6754	18.8	0.18	8432
S6	OGLE004744.17-731812.6	0.4672	18.59	0.1	8937
S7	OGLE004849.85-725554.8	0.4333	18.52	0.15	8299
S8	OGLE004941.64-730855.4	0.6152	18.51	0.16	8559
S9	OGLE005020.27-732404.1	0.6159	17.36	-0.07	10729
S10	OGLE005109.79-732308.2	0.6317	16.62	-0.18	13680
S11	OGLE005144.08-723324.7	0.5011	17.22	-0.11	11266
S12	OGLE005251.69-725103.7	0.7189	18.79	0.1	8936
S13	OGLE005303.52-725711.5	0.6960	18.34	-0.02	10058
S14	OGLE005412.66-724209.1	0.4969	17.25	0	9790
S15	OGLE005505.44-724053.6	0.6141	17.7	0.01	9703
S16	OGLE005642.21-725856.0	0.6179	17.26	-0.03	10193
S17	OGLE005645.52-730850.9	0.6652	18.53	0.11	8874
S18	OGLE010254.36-722500.3	0.6852	16.58	-0.11	11266
S19	OGLE010836.56-722657.0	0.5813	16.96	-0.02	10058
S20	OGLE010907.46-722434.4	0.7464	17.61	-0.07	10729

variables were assumed to be non-contact in nature (mode 2) and later we found that, for all the variables the solutions were converging to contact binary systems and hence mode 3 was used.

The parameters adopted in the solutions are as follows: the effective temperature for primary star is taken on the basis of V-I values and using Allen's (2000) table. Initially the secondary component effective temperature ($T_{e,c}$) was assumed to be equal to primary component's temperature. The values of limb darkening coefficients, x_h & x_c = 0.80 for I band were taken from Al-Naimy (1978). As the components possess high temperatures where radiative envelopes dominate, the values A=1, g=1 were assumed.

The mass-ratio parameter is unknown for the respective systems and hence in order to constrain it we adopted the following procedure. Initially the mean effective temperature of cool star T_c, the dimensionless surface potentials Ω_h=Ω_c, monochromatic luminosity L_h and orbital inclination i along with mass ratio (q) are adopted as adjustable parameters. Figures 1 and 2 show the weighted sum of square of residuals $\Sigma\omega$(O-C)^2 for assumed mass ratio values. The results of the computed solutions are shown in Tables 2, 3, 4 and 5. We have used the LC program incorporating the final parameters resulting from the DC program, to obtain the theoretical light curves. The observed and theoretical light curves for each variable are shown in Figures 3, 4, 5, 6 and 7.

4. Discussions and results

We have selected twenty hot variables in SMC, in order to derive the photometric elements. The selected variables have periods less than 0.8 days and spectral types ranging from B8 to F0 based on their V-I colour. Siwak et al. (2011) have studied hot contact binaries with large temperature

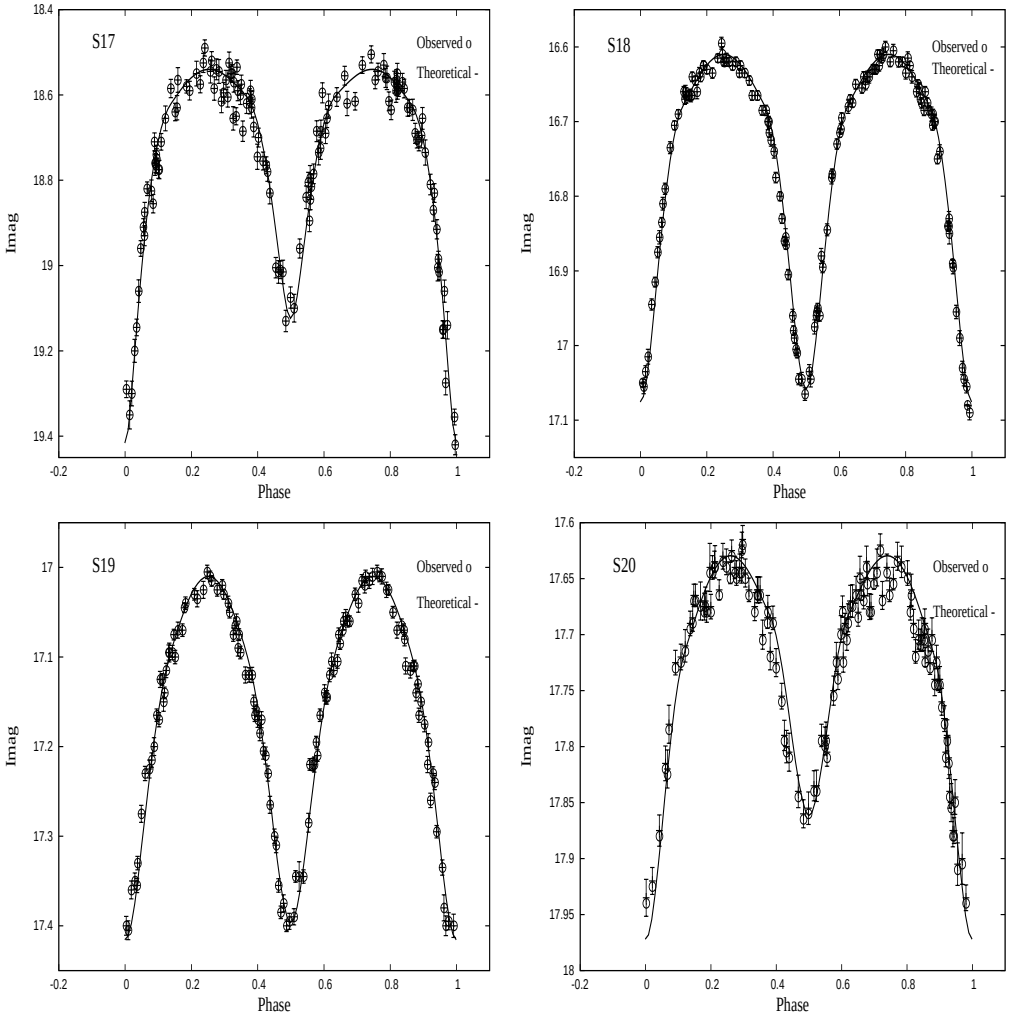

Figure 7. The figures show the best fits to the I passband light curves for the variables S17, S18, S19 and S20 in SMC.

differences and the hottest source was DO Cas with the primary's component temperature ∼ 9000 K. In our sample, variables have relatively much higher temperature (see Tables 1, 2, 3 and 4) and since such hot variables are not studied, became the motivation of the present work. The W-D program was used to derive the photometric solutions for the respective variables. The photometric solutions suggest that all the variables belong to marginal over contact or over contact binary systems. All the variables fall in the new classification scheme H sub-type (Csizmadia & Klagyivik 2004).

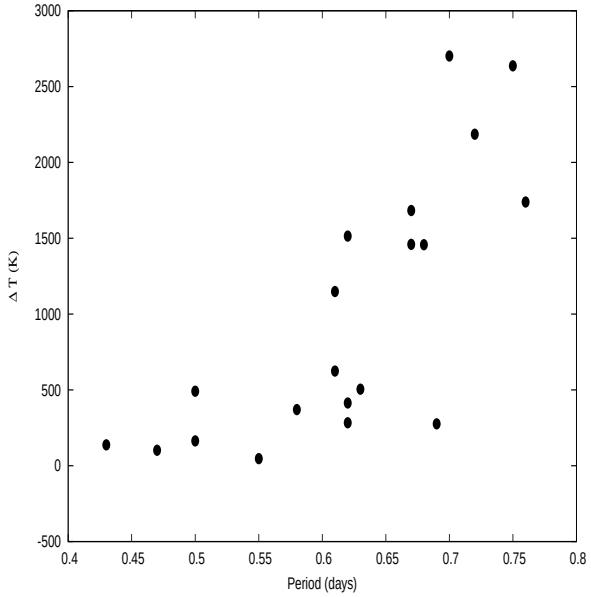

Figure 8. The variation of period vs temperature difference for the selected sample is shown.

Table 2. The Photometric elements obtained for five variables by using W-D method. "a" denotes the fixed parameter during the fit, h (primary) and c (secondary) are hot and cool components and Δ T is the temperature difference between primary and secondary component.

Element		S1	S2	S3	S4	S5
Period (days)		0.5546	0.6651	0.7625	0.6057	0.6754
$T_{e,h}{}^a$ K		9351	8004	11400	9088	8432
$T_{e,c}$ K		9304±338	6321±120	9661±137	7937±165	6975±158
ΔT K		47	1683	1739	1149	1457
q^a		0.91±0.07	1.08±0.13	1.48±0.06	1.02±0.09	0.73±0.17
i^o		64.29±1.09	78.87±0.68	72.12±0.36	73.87±0.62	82.77±1.90
Ω		3.7183±0.1127	4.1657±0.2356	4.6550±0.0987	3.8937±0.1472	3.3847±0.3166
fill-out factor		0.2311	0.7623	0.5199	0.1549	0.6689
r_h	pole	0.3640±0.0074	0.3661±0.0059	0.3363±0.0050	0.3586±0.0076	0.3845±0.0305
	side	0.3827±0.0092	0.3873±0.0075	0.3539±0.0062	0.3773±0.0095	0.4059±0.0387
	back	0.4134±0.0133	0.4284±0.0122	0.3939±0.0105	0.4106±0.0147	0.4363±0.0553
r_c	pole	0.3482±0.0076	0.3796±0.0057	0.4013±0.0044	0.3623±0.0075	0.3311±0.0337
	side	0.3653±0.0093	0.4024±0.0074	0.4264±0.0057	0.3814±0.0095	0.3469±0.0414
	back	0.3966±0.0138	0.4423±0.0116	0.4616±0.0085	0.4144±0.0145	0.3795±0.0646
L_h		0.4718	0.6192	0.4702	0.5572	0.6739
L_c		0.5282	0.3808	0.5298	0.4428	0.3261
L_3		-	-	-	-	-
x_h		0.80±0.05	0.80±0.05	0.80±0.05	0.80±0.05	0.80±0.05
x_c		0.80±0.05	0.80±0.05	0.80±0.05	0.80±0.05	0.80±0.05
$\Sigma w(o-c)^2$		0.01521	0.02857	0.00495	0.01812	0.05677
Spectral type		A2-A0	A5	B8	A2-A0	A5-A2
A_h^a		1.0	1.0	1.0	1.0	1.0
A_c^a		1.0	1.0	1.0	1.0	1.0

Table 3. The Photometric elements obtained for five variables by using W-D method. "a" denotes the fixed parameter during the fit, h (primary) and c (secondary) are hot and cool components and Δ T is the temperature difference between primary and secondary component.

Element		S6	S7	S8	S9	S10
Period (days)		0.4672	0.4333	0.6152	0.6159	0.6317
$T_{e,h}{}^a$ K		8937	8299	8559	10729	13680
$T_{e,c}$ K		9039±222	8161±189	7045±204	10446±172	13175±291
ΔT K		102	138	1514	283	505
q^a		0.81±0.20	0.81±0.03	1.05±0.09	0.98±0.03	1.56±0.01
i^o		77.22±0.79	72.29±0.90	72.70±0.91	68.18±0.44	63.16±0.43
Ω		3.5036±0.1174	3.6189±0.2012	3.8701±0.1640	3.7932±0.0491	4.5484±0.0230
fill-out factor		0.1528	0.3554	0.2850	0.0795	0.0386
r_h	pole	0.3758±0.0142	0.3745±0.0043	0.3474±0.0219	0.3619±0.0077	0.3413±0.0023
	side	0.3962±0.0180	0.3947±0.0054	0.3639±0.0268	0.3812±0.0097	0.3607±0.0028
	back	0.4272±0.0260	0.4255±0.0077	0.3928±0.0389	0.4151±0.0145	0.4084±0.0051
r_c	pole	0.3403±0.0152	0.3406±0.0045	0.3556±0.0216	0.3619±0.0077	0.4146±0.0021
	side	0.3569±0.0187	0.3572±0.0055	0.3729±0.0266	0.3812±0.0097	0.4430±0.0027
	back	0.3894±0.0287	0.3894±0.0083	0.4016±0.0381	0.4151±0.0145	0.4828±0.0041
L_h		0.5419	0.5525	0.5912	0.5106	0.4175
L_c		0.4581	0.4475	0.4088	0.4894	0.5825
L_3		-	-	-	-	-
x_h		0.80±0.05	0.80±0.05	0.80±0.05	0.80±0.05	0.80±0.05
x_c		0.80±0.05	0.80±0.05	0.80±0.05	0.80±0.05	0.80±0.05
$\Sigma w(o\text{-}c)^2$		0.02601	0.02627	0.03584	0.00579	0.00186
Spectral type		A5-A2	A5-A2	A5-A2	A0-B8	B8-B5
A_h^a		1.0	1.0	1.0	1.0	1.0
A_c^a		1.0	1.0	1.0	1.0	1.0

From the analysis of our sample, we found that mass ratios have high values and for a few systems, q > 1, implying that mass is transferring from secondary to primary component. The photometric solutions show that the variables S2, S3, S4, S5, S8, S12, S13, S17 and S20 to have high temperature differences (Δ T > 1000 K) between the primary and secondary components and S10, S11, S15, S16 and S19 to have relatively lower temperature differences (Δ T > 400-600 K). Such temperature differences are often observed in EB-type systems, also referred as poor thermal contact (PTC) systems (Deb et al. 2011; Martignoni et al. 2009; Rucinski & Duerbeck 1997). These EB-type systems are important and interesting as they are supposed to undergo thermal relaxation oscillation (TRO) (Flannery 1976; Lucy 1976; Robertson & Eggleton 1977; Li et al. 2004a,b; Li et al. 2005). This theory suggests that the contact binary system undergoes oscillation between the contact and non-contact/semi-detached phases on thermal timescales ($\sim 10^7$ yr) because of non-thermal equilibrium. During the non-contact phase, the degree of thermal contact among the two components is low and the system exhibits EB-type light curve variability. Qian (2001) studied 27 hot contact binaries and suggested that except one system all of them showed period increasing trend i.e., mass transferring is occurring from secondary to primary component. However two other contact binaries FT Lup and CN And show period decreasing trend (Kreiner et al. 2001). Fig. 8 shows the variation of temperature difference (Δ T) over period for our sample. It is clearly seen that the Δ T increases along with the period, strongly agreeing with the result of Qian (2001) for hot contact binaries.

These systems are relatively more important compared with cool contact binaries because of low levels of magnetic activity and these closely follow thermal relaxation oscillation (TRO)

Table 4. The Photometric elements obtained for five variables by using W-D method. "a" denotes the fixed parameter during the fit, h (primary) and c (secondary) are hot and cool components and Δ T is the temperature difference between primary and secondary component.

Element		S11	S12	S13	S14	S15
Period (days)		0.5011	0.7189	0.6960	0.4969	0.6141
$T_{e,h}{}^a$ K		11266	8936	10058	9790	9703
$T_{e,c}$ K		10775±273	6750±172	7356±130	9626±162	9079±105
ΔT K		491	2186	2702	164	624
q^a		1.61±0.02	0.98±0.13	1.31±0.12	0.81±0.03	0.91±0.03
i^o		64.26±0.39	75.21±1.00	78.41±0.72	82.04±0.62	82.65±0.46
Ω		4.6826±0.0225	3.8557±0.2253	4.4186±0.2084	3.4185±0.0681	3.5962±0.0377
fill-out factor		0.0116	0.2865	0.2677	0.0034	0.0213
r_h	pole	0.3177±0.0024	0.3580±0.0139	0.3354±0.0093	0.3998±0.0109	0.3685±0.0069
	side	0.3322±0.0029	0.3762±0.0173	0.3515±0.0114	0.4267±0.0146	0.3884±0.0088
	back	0.3648±0.0047	0.4072±0.0257	0.3841±0.0174	0.4720±0.0245	0.4214±0.0133
r_c	pole	0.3969±0.0020	0.3550±0.0140	0.3804±0.0088	0.3654±0.0119	0.3537±0.0071
	side	0.4199±0.0026	0.3728±0.0174	0.4013±0.0111	0.3880±0.0155	0.3719±0.0090
	back	0.4493±0.0037	0.4040±0.0259	0.4319±0.0157	0.4379±0.0288	0.4057±0.0140
L_h		0.4081	0.6503	0.5789	0.5515	0.5485
L_c		0.5919	0.3497	0.4211	0.4485	0.4515
L_3		-	-	-	-	-
x_h		0.80±0.05	0.80±0.05	0.80±0.05	0.80±0.05	0.80±0.05
x_c		0.80±0.05	0.80±0.05	0.80±0.05	0.80±0.05	0.80±0.05
$\Sigma w(o\text{-}c)^2$		0.00570	0.03913	0.02673	0.02189	0.00977
Spectral type		A0-B8	A5-A2	A0-B8	A0	A0
A_h^a		1.0	1.0	1.0	1.0	1.0
A_c^a		1.0	1.0	1.0	1.0	1.0

Table 5. The Photometric elements obtained for five variables by using W-D method. "a" denotes the fixed parameter during the fit, h (primary) and c (secondary) are hot and cool components and Δ T is the temperature difference between primary and secondary components.

Element		S16	S17	S18	S19	S20
Period (days)		0.6179	0.6652	0.6852	0.5813	0.7464
$T_{e,h}{}^a$ K		10193	8874	11266	10058	10729
$T_{e,c}$ K		9779±148	7414±113	10990±98	9688±144	8092±157
ΔT K		414	1460	276	370	2637
q^a		1.09±0.06	0.71±0.09	1.10±0.04	1.10±0.03	1.00±0.03
i^o		72.42±0.41	84.95±1.52	74.39±0.24	68.63±0.36	65.58±0.56
Ω		3.9976±0.1056	3.3627±0.1807	4.0592±0.0695	3.9155±0.0554	3.9466±0.0684
fill-out factor		0.4086	0.2497	0.2108	0.0085	0.36192
r_h	pole	0.3667±0.0036	0.3869±0.0106	0.3655±0.0037	0.3482±0.0016	0.3596±0.0069
	side	0.3881±0.0046	0.4086±0.0135	0.3865±0.0048	0.3653±0.0019	0.3786±0.0086
	back	0.4299±0.0075	0.4389±0.0192	0.4268±0.0078	0.3965±0.0028	0.4127±0.0129
r_c	pole	0.3810±0.0036	0.3290±0.0117	0.3783±0.0036	0.3641±0.0016	0.3645±0.0068
	side	0.4041±0.0046	0.3445±0.0144	0.4007±0.0047	0.3828±0.0019	0.3840±0.0085
	back	0.4446±0.0072	0.3773±0.0225	0.4400±0.0075	0.4135±0.0027	0.4179±0.0128
L_h		0.4960	0.6679	0.4904	0.4932	0.6130
L_c		0.5040	0.3321	0.5096	0.5068	0.3870
L_3		-	-	-	-	-
x_h		0.80±0.05	0.80±0.05	0.80±0.05	0.80±0.05	0.80±0.05
x_c		0.80±0.05	0.80±0.05	0.80±0.05	0.80±0.05	0.80±0.05
$\Sigma w(o\text{-}c)^2$		0.00492	0.01944	0.00235	0.00397	0.00413
Spectral type		A0-B8	A5-A2	B8	A0-B8	A0-B8
A_h^a		1.0	1.0	1.0	1.0	1.0
A_c^a		1.0	1.0	1.0	1.0	1.0

models. In cool contact binaries it is both the TRO and angular momentum loss (AML) mechanisms via magnetic field lines which complicates the understanding of these systems. Recently, Siwak et al. (2011) studied 12 contact binaries with large temperature differences and found hot spot on secondary components on few sources which is an indication of accretion effects and strongly argues in favour of semi-detached configurations. However they have not found a semi-detached configuration from light curve or radial velocity modeling of the observed light curves. Since our sample consists of very hot stars, we argue that stellar wind might play a key role in mass loss (ML) which is generally of the order of $\sim 10^{-6}$ $M_{\odot}$ and would also affect the total dynamics of the contact binary system. Such high temperature contact binary systems are rare and are crucial to understand their structure and evolution in terms of TRO.

We found that, few systems have low inclination values (see the tables) which are often seen in other contact binaries. However, the W-D solution may not give correct solution for such partial eclipsing binaries (Rucinski 2001) and hence the corresponding results are the preliminary solutions to unveil the nature of the respective variables. Since mass ratio is intended to be the most important parameter, spectroscopic radial velocity observations and long-term photometric monitoring are necessary in order to understand the hot contact binaries.

Acknowledgements

The authors acknowledge the anonymous referees for their useful comments.

References

Allen C. W., 2000, in Arthur N. Cox (ed.), Allen's Astrophysical Quantities, Springer-Verlag, NY
Al-Naimy H.M., 1978, Ap&SS, 53, 181
Csizmadia Sz., Klagyivik P., 2004, A&A, 426, 1001
Deb S., Singh H. P., 2011, MNRAS, 412, 1787
Falnnery B.P., 1976, ApJ, 205, 217
Guinan E. F. 1993, in New Frontiers in Binary Star Research, ed. K.-C. Leung, I.-S. Nha, ASP Conf. Ser., 38, 1
Hilditch R. W., 2001, An Introduction to Close Binary Stars, Cambridge University Press, Cambridge
Kaluzny J., Stanek K. Z., Krockenberger M., et al. 1998, AJ, 115, 1016
Kreiner J. M., Kim Ch. H., 2001, An Atlas of O-C Diagrams of Eclipsing Binary Stars, Wydawnictwo Naukowe AP, Krakow
Li L., Han Z., Zhang, F., 2004a, MNRAS, 351, 137
Li L., Han Z., Zhang F., 2004b, MNRAS, 355, 1383
Li L., Han Z., Zhang F., 2005, MNRAS, 360, 272
Lopez-Morales M., 2007, ApJ, 660, 732
Lucy L. B., 1968, ApJ, 151, 1123
Lucy L. B., 1976, ApJ, 205, 208
Martignoni M., Acerbi F., Barani C., 2009, RAA, 9, 1270
Munari U., Dallaporta S., Siviero A., et al. 2004, A&A, 418, L31
Paczynski B., Sienkiewicz R., Szczygiel D. M., 2007, MNRAS, 378, 961

Popper D. M., 1967, ARA&A, 5, 85
Qian J. J, Liu H. Y., 2001, Journal Of Applied Physics, 90, 4
Ravi Kiron Y., Sriram K., Vivekananda Rao P., 2012, BASI , 40, 51
Ravi Kiron Y., Sriram K., Vivekananda Rao P., 2011a, BASI , 39, 247
Ravi Kiron Y., Sriram K., Vivekananda Rao P., 2011b, RAA , 11, 1067
Ravi Kiron Y., Sriram K., Vivekananda Rao P., 2011c, RAA, 11, 1469
Reegan P., 2007, A&A, 467, 1353
Ribas I., Jordi C., Vilardell F., et al. 2005, ApJ, 635, L37
Robertson J. A., Eggleton P. P., 1977, MNRAS, 179, 359
Rucinski S. M., 2001, AJ, 122, 1007
Rucinski S. M., Duerbeck H. W. 1997, PASP, 109, 1340
Rukmini J., Vivekananda Rao P., 2002, BASI, 30, 665
Rukmini J., Vivekananda Rao P., Sriram K., 2005, Ap&SS, 299, 109
Siwak M. Zola, S., Wierzbowska K. D., 2011, Acta Astron., 61, 305
Sriram K., Ravi Kiron Y., Vivekananda Rao P., 2009, RAA, 9, 1149
Sriram K., Vivekananda Rao P., 2010, RAA, 10, 159
Shanti Priya D., Sriram K., Vivekananda Rao P., 2011, RAA, 2, 175
Stepien K., 2009, MNRAS, 397, 857
Torres, G., Andersen, J., Gimenez, 2009, A&ARv, 13
Udalski A., Kubiak M., Szymanski M., 1997, Acta Astron. 47, 319
Van Hamme W., Wilson R. E., 2003, ASPC, 298, 323
Wilson R., E., Devinney E., J., 1971, ApJ, 166, 605
Wyrzykowski L., Udalski A., Kubiak M., Szymanski M., Zebrun K., Szewczyk O., 2003, Acta Astron., 53, 1
Yakut K., Eggleton P., 2005, ApJ, 629, 1055